Korean J. Chem. Eng., 32(7), 1207-1217 (2015)
DOI: 10.1007/s11814-015-0071-5

pISSN: 0256-1115
eISSN: 1975-7220

REVIEW PAPER

Modeling and simulation of biopolymer networks: Classification of the cytoskeleton models according to multiple scales

Nilanjana Banerjee and Joontaek Park†

The Department of Chemical and Biochemical Engineering, Missouri University of Science and Technology, Rolla, MO 65409, USA

(*Received 4 February 2015 • accepted 7 April 2015*)

Abstract−We reviewed numerical/analytical models for describing rheological properties and mechanical behaviors of biopolymer networks with a focus on the cytoskeleton, a major component of a living cell. The cytoskeleton models are classified into three categories: the cell-scale continuum-based model, the structure-based model, and the polymer-based model, according to the length scales of the phenomena of interest. The criteria for classification of the models are modified and extended from those used by Mofrad [M. R. K. Mofrad, *Annual Rev. Fluid Mech.* **41**, 433 (2009)]. The main principles and characteristics of each model are summarized and discussed by comparison with each other. Since the stress-deformation relation of cytoskeleton is dependent on the length scale of stress elements, our model classification helps systematic understanding of biopolymer network modeling.

Keywords: Cytoskeleton, Biopolymer Network, Actin Filament, Cell Dynamics, Multiscale Modeling

INTRODUCTION

Recent studies in medicine have elucidated the need to understand how the structures of biopolymers and the various physical forces acting on them contribute to the synthesis, growth, transportation, information processing and functioning of living cells and tissues. Many of these forces and their effects have been identified and studied, such as hemodynamic shear stress on vascular tissues, inspiratory pressure on lung functions, and tension on skin aging [1]. In addition, numerous diseases, including tumors, lung cancer, emphysema, neuro-degeneration, pulmonary fibrosis, etc. [2-4], have been associated with the change of these physical forces and, subsequently, the biopolymer structures. These physical forces have also been found to be vital for cellular and genetic regulation in the living body [5].

Living cells dynamically respond to any mechanical perturbations in their environment solely by altering the cytoskeleton configuration and functioning [6,7]. The cytoskeleton is a network of protein tubules present inside a cell that is responsible for cellular structure, shape, movement and growth. Cells are adhered to a scaffold called the extra-cellular matrix. During the process of cell growth and movement, the cellular forces in the scaffold and inside the cell are balanced by the cytoskeleton [8-11]. Even the interactions between two adjacent cells are affected by the mechanical behavior of the cytoskeleton [12]. Thus it is imperative to identify the various mechanical forces and analyze their effects on the structure and behaviors of the cytoskeleton in order to understand cell functioning and abnormalities. This knowledge will lead to a better understanding of the causes of disease and corresponding cures.

†To whom correspondence should be addressed.
E-mail: parkjoon@mst.edu

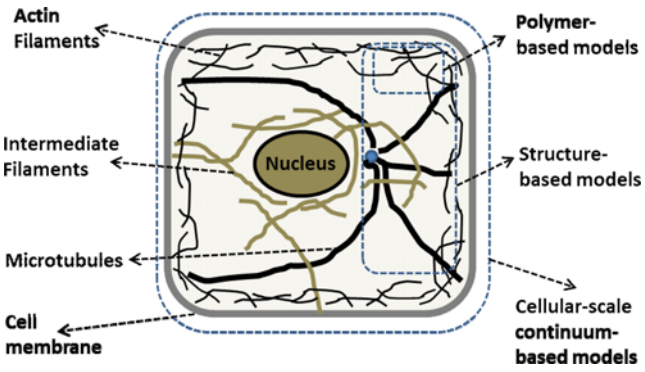

Fig. 1. Schematic diagram which shows the structural components of the cytoskeleton in a typical eukaryotic cell and the length scales for each group of models.

There have been numerous efforts to model the relationships between the structure of the cytoskeleton and its rheological properties and mechanical behaviors. However, due to the cytoskeleton's complex structure and heterogeneous components, no single approach has been able to accurately encompass all of its various behaviors. As shown in Fig. 1, the cytoskeleton network is composed of three main highly entangled protein structures: actin filaments, microtubules and intermediate filaments. These components together are responsible for the properties and mechanics of the cells [13].

The actin filament (or F-actin), a filamentous form of monomeric G-actin protein, is the major component of the cytoskeleton, comprising up to 10% of the total cellular protein mass [14]. It has a persistent length of about 15-17 μm [15]. The F-actin further cross-links to create a bundle or an orthogonal cytoskeleton network structure by the cross-linking of actin binding proteins [15-21]. The F-actin filaments are also continuously undergoing polym-

erization and depolymerization, leading to an active network structure [15,22-24]. These cross-linkers and the degree of crosslinking also lead to strain stiffening behavior exhibited by the F-actin [13, 25].

Microtubules, the second major component of the cytoskeleton network, exhibit hollow cylindrical shapes composed of monomers α and β-tubulin with persistent lengths of 6 mm [13,15]. They have higher bending stiffness, are more active in nature than actin filaments, and continuously undergo polymerization and depolymerization [25,26]. The microtubules are known to be the compressive load-bearing component of the network as balanced against the tensed actin and intermediate filaments [27].

The intermediate filaments (persistence length ~1 μm) are the least well studied of the three components of cytoskeleton [13,15]. They, along with the F-actin, act as the tension-bearing components under deformation and have a rope-like structure consisting of different proteins [12-13,25]. They are more stable compared to F-actin and microtubules and can withstand higher stresses and strains before rupture [25].

The dynamics and properties of the cytoskeleton result from the collective actions of the aforementioned components at various time and length scales. Therefore, successful modeling of the cytoskeleton requires proper approximation of the behaviors and properties of those structural elements for the time and length scales of the phenomena of interest. The length scale is important for thermal and mechanical effects. However, biological effects or structural reorganization, including polymerization/depolymerization, must consider both length and time scales. For example, the stress-deformation behaviors within a time scale range where there is no structural reorganization or polymerization/depolymerization are referred to as "passive dynamics," whereas "active dynamics" are related to biological responses at longer time scales [13].

This review paper classifies numerous analytical and numerical models used to analyze cytoskeleton behaviors and properties into three groups according to length scales: cell-scale continuum-based models, structure-based models, and polymer-based models, as shown in Fig. 1. We focus on models used to analyze the passive dynamics of the cytoskeleton. Length scales of individual cell mechanical properties range from atomistic to the macroscopic cell level. Note that we exclude models that work at the scale of collective cell motions (>10 μm).

Our classification is adapted from that used by Mofrad's review in 2009 [13]. Models which describe the dynamic behaviors of a single cell as an elastic continuum medium are classified as "cell-scale continuum-based models." Mofrad named similar models "continuum-based models," but we add "cell-scale" (typically around 10 μm [28]) to distinguish them from continuum approaches at smaller scales [28]. Structure-based models consider cytoskeleton properties with discrete representative volume elements (RVE) which approximate the stress-deformation relationship among structural components (typically between 1 and 10 μm [28]). As this model name was used in Chen's review in 2014 [29], these models encompass the groups of "tensegrity models" as classified in Mofrad [13], the models reviewed by Chen and co-workers in 2012 [30], and the continuum polymer network models summarized in a review by Unterberger and Holzapfel in 2014 [28]. The "polymer-based model" explains the cytoskeleton properties in terms of polymer network structures (typically around 1 μm [28]) or a single polymer molecule (less than 10 nm [28]), as in Mofrad [13].

Many reviews have summarized various models for cellular and cytoskeleton dynamics using different approaches. As mentioned, Mofrad provided a unified insight into the overall cytoskeleton rheology and experimental techniques [13]. However, additional structure-based and polymer-based models have subsequently been added to other reviews. Chen and co-workers summarized models by focusing particularly on the structure-based models [30]. Chen's review classified models into continuum-based and structure-based models. However, the author specifically arranged continuum-based models related to indentation experiments into another separate group: nanoindentation models. [29]. Nava and co-workers [31] and Moeendarbary and Harris [32] have unified various models ranging from cell mechanics (>10 μm) to cytoskeleton behaviors (~1 μm). The former, which is mostly related to mechanics of adherent cells, proposed a model classification that included only continuum-based models and structure-based models (they used the terms of continuum model and microstructural model). The latter models depict various cell phenomena at different time scales and length scales, but do not provide much detail on cytoskeletons. There were other reviews [28,33,34] which mainly emphasized polymer-based models (from molecular level to network scale), but did not provide much discussion of cell-scale and structure-based models.

Our aim is to provide a systematic understanding of cytoskeleton models in terms of length scales, which determine the stress-deformation relation of the cytoskeleton. This paper summarizes the underlying principles, main applications, and advantages and disadvantages of cytoskeleton models in each classified length scale group.

CELL-SCALE CONTINUUM-BASED MODELS (~10 μm)

The cell-scale continuum-based models describe the mechanical/rheological behaviors and properties of a cell at cellular length scales (typically ~10 μm), which is larger than the typical distance between different cell components [28]), by assuming that cell cytoplasm is a homogeneous and continuous medium. These models are usually used for the simulation of cell motions (migration, spreading, etc.) or experiments for cell property measurements [35]. Based on the level of simplification and the behaviors of interest, these models can be further classified into elastic/viscoelastic models, multi-phasic models and soft glassy models.

1. Elastic/Viscoelastic Models

Elastic/viscoelastic continuum-based models utilize Cauchy's momentum equation as well as constitutive equations that represent the stress-strain behavior of the cytoskeleton as a homogeneous elastic or viscoelastic medium [13]. A cell cytoplasm is discretized into small computational units (mesh) to solve those model equations by the finite element method with necessary boundary conditions. The major application of this approach is for analyzing and evaluating the cells' experimentally measured *in vivo* and *in vitro* force levels and their effects on cell behaviors [36]. It gives adequate results when measuring the cell deformation macroscopically [37,38].

These models are classified into elastic models or viscoelastic

models, depending on the dynamic time scale of the cellular behavior of interest [13]. An elastic model is sufficient to describe small deformations following Hook's law, whereas a nonlinear elastic model, such as the Gaussian model, is required for larger deformations [29]. However, the elastic models are only suitable for modeling cell material properties and cell dynamic behaviors at limited time scales (near equilibrium) due to their oversimplification [29,31].

The time-dependent stress-strain behaviors can be described by the viscoelastic models that utilize typical viscoelastic constitutive equations, such as typical or modified Maxwell models [31,32]. Viscoelastic models have been able to predict the cellular mechanics for blood cells, which are under continuous shear and high mechanical perturbations, as well as for adherent cells such as epithelial and endothelial cells [39]. Recently, a 2D viscoelastic model was used to simulate cell migration in a microchannel [39]. A recent 3D constitutive model was extended to simulate lipid bilayer-cytoskeleton coupling in an erythrocyte membrane [40].

2. Multiphasic Model

The multiphasic continuum model was first proposed by Guilak and co-workers, based on the idea that the viscoelastic behaviors of cells can be attributed to the intrinsic viscoelastic property of the cytoskeleton (solid phase in cytoplasm), the fluid viscosity of the interstitial fluid (cytosol: water with ions), and the solid-fluid interaction within a cell [41]. The basic approach of the biphasic cell model [42] can be extended to a more realistic physical representation of a cell by adding more phases. Therefore, the biphasic approach requires constitutive stress-strain equations in each phase as well as additional momentum and mass conservation equations over those phases. For example, the triphasic model considers a viscous liquid phase, an elastic solid phase, and an ionic phase, where two stress-deformation equations are required for the liquid and solid phases and an additional equation exists for the osmotic pressure in the ionic phase [43,44].

Time or deformation rate-dependent response to stress can be described by the poro-elastic or poro-viscoelastic concept, which views the cytoplasm as a wetted porous solid [45-47]. Under this context, the cell viscoelasticity is a measure of the time scale (function of the poro-diffusivity, which is proportional to a combined variable of elastic modulus of the solid phase, porous size, and the fluid phase viscosity) needed for the redistribution of the intracellular fluids and cell response under mechanical perturbations. As the poro-diffusivity increases, the relaxation of the cell gets faster [32].

A combination of the above models with the structure-based models can be used to study the phase interactions and cell mechanics. The multiphasic approach can more accurately predict the cell rheological behaviors, such as creep response of the cell [48] and the chondrocyte mechanics [49]. However, one of the major disadvantages of these models is the increased number of estimated parameters and the increase in complexity of the model [32,41].

3. Soft Glassy Models

The soft glassy rheology model [50,51] (also referred as power-law rheology [29]) was initially proposed by Sollich and co-workers [52,53], describing soft glassy materials with weak dependence of storage (G′) and loss (G″) moduli on frequency, ω Soft glassy materials generally have a disordered structure of aggregated discrete components (foams, pastes, colloids, etc.) that interact weakly. They usually have low moduli in the range of Pa to kPa, and are not thermodynamically stable. Based on the above observations of the resemblance of the cytoskeleton to soft glassy materials, the soft glassy rheology was proposed as another interpretation of the continuum-based cytoskeleton model to explain how the macroscopic cellular response is related to the localized structural rearrangements caused by meta-stability and disordered structure [32,50,51]. This model can adequately predict the frequency dependency of elastic and loss moduli for all animal tissue types, including the smooth muscles in human airway, endothelial and epithelial cells, for a wide time range of ~0.001-100 sec using a universal parameter called a noise temperature. However, microscopic interpretation of this parameter has not been performed [50].

4. Discussion of the Cell-scale Continuum-based Models

The aforementioned cell-scale continuum-based models have been widely used for simulation of whole cell behavior as well as for cell material property experiments. According to the conditions of the behaviors of interest, different models can be chosen. For example, even for simulations of the same micropipette aspiration experiments, different models have been chosen according to the ranges of deformation and time [48,54,55].

There are some major disadvantages with all of the above continuum-based models. First, these models emphasize macroscopic cellular behaviors and dynamics. Microstructure and individual cytoskeleton component behaviors are not considered by approximation at the continuum level. For example, the effects of actin cross-linkers, thermal fluctuations, and polymerization/depolymerization are neglected. Therefore, the interpretation of the molecular level interactions is not allowed. Additionally, the macroscopic models cannot predict and understand the pre-stressed phenomenon observed in the cytoskeleton network [56]. The structure-based models and the polymer-based models, which will be discussed in the subsequent sections, portray a better understanding of cytoskeleton properties and behaviors from a microstructural point of view.

STRUCTURE-BASED MODEL (1~10 μm)

Structure-based models utilize discrete structural elements, which represent the individual stress-strain relationships among the microstructural components of the cytoskeleton, to describe the rheological properties and mechanical behaviors of the cytoskeleton [29, 32]. Since the heterogeneity of the cytoskeleton is considered through the microstructural stress elements, these models can describe some cell behaviors that cannot be simulated by the cell-scale continuum-based models, such as stability of the cell shape and cell stiffness [56]. The structure-based models can be further categorized into pre-stress (pre-existing tensile stress) models and semi-flexibility models. Pre-stress models, which include the cortical membrane model, the tensed cable nets model, and the tensegrity (cable and strut) models, consider pre-stress in the intercellular force balance to predict cell shape [56]. Note here that some reviews, such as by Mofrad [13], named all pre-stress models as tensegrity models. Semi-flexibility models include open cell foam models, the semi-flexible network element model ("element" is added to be distinguished from other polymer-based network models), and contin-

uum polymer network models, which utilize RVE to represent the coarse-grained semi-flexible actin network [30]. The pre-stress model is important because the pre-stress is related to the cell shape stability and the cell stiffness [56]. The semi-flexibility model relates the bending ability of actin filaments with cell behaviors, such as strain hardening [30,31]. Since the stress elements of these models consider the cytoskeleton components, the element length scales are considered to be smaller than cell scale (<10 μm) [28]. However, since the stress element is still an imaginary representation of the actual polymer network, the element length scale is considered to be larger than the polymer network scale (>1 μm) [31,56]. These models consider affine approximation (local deformation is the same as the macroscopic deformation) of the discrete elements, allowing continuum interpretations of the deformations, resulting in less numerical and computational complexity than the polymer-based models [56].

1. Cortical Membrane Model

This model assumes that the stress bearing elements of the cytoskeleton are restricted within a thin or several thin distinctive cortical layers with the stress balanced either completely by the pressurized cytoplasm itself, or by the cytoplasm and extracellular matrix together [57]. This model can also predict the linear stress and cell stiffness relationship and give a good approximation for suspended cell (e.g., blood cells) and non-adherent cell behavior [58,59]. The major disadvantage of this model is that its primary assumption, that the resistance to cell shape alteration is provided by a thin cortical layer, cannot be applied to adherent cells [60]. Thus, the limitation of this model inspired the shell-like 3D pre-stress models in the next section [30,56].

2. Tensed Cable Nets Models

This concept models a network completely constituted of tensile cable elements (linear-elastic springs) without the balanced compression in the microtubules. The pre-stress is maintained and supported by the external extracellular matrix. The model predicts a linear relationship between stiffness and stress when the cable tension is constant; otherwise, the trend is non-linear [56]. As in the cortical membrane model, the pre-stress in the cortical membrane can be simulated with 2D tensed cable nets [59,61,62]. One example of a typical 2D cable net (reinforced squared net) is shown in Fig. 2. In the case of the behavior of suspended cells, such as blood cells, this model provides very good agreement with the experimental observations; however, the behaviors of adherent cells, such as cell spreading and cell migration, require more complicated 3D models for better simulation [30,56].

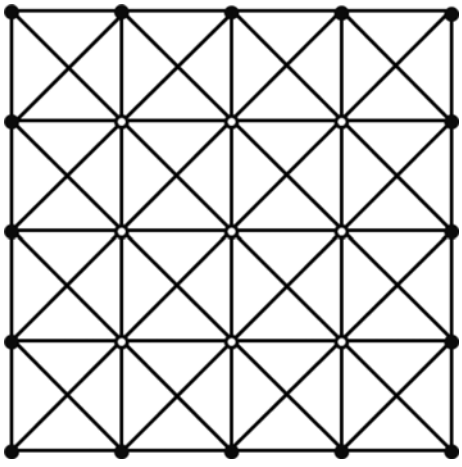

Fig. 2. A typical example of 2D tensed cable nets models: Reinforced squared nets (Redrawn from [61,62]).

The 3D tensed cable nets models construct 3D cable networks with uncrossed free-sliding joints as well as pin joints [63,64]. The pre-stress is equal to the sum of all the tensile forces in the cables across a cross-sectional area [63,65]. This model is also able to predict some of the mechanical properties, such as Young's modulus, of the cytoskeleton and has good accordance with micropipette aspiration experiments. It also provides better interpretations of cell mechanics compared to the open cell foam models, which will be introduced later [30]. Major disadvantages with these models are that they do not include anything about compressed microtubules and still have limited ability to predict the behavior for adherent cells [27,31,56].

3. Tensegrity (Cable-strut) Models

The tensional integrity, or tensegrity, model employs a discrete network of self-stabilizing pre-stressed tension bearing components (actin and intermediate tubules) which are balanced by locally compressed units (microtubules), each subjected to mechanical equilibrium and geometric deformation [10,27,66]. *In vivo* probing has clarified that the actin filaments are the stiffest of all cytoskeleton components with a linear shape, whereas the microtubules appear curved. Thus, the principal assumption of this model is that actin and intermediate tubules are the stress bearing components but the microtubules resist compression, which is in accordance with the above observations [10,67,68]. The stress element of this model is based on variations of Buckminster Fuller's tensional integrity structure, proposed in 1961 [69]. This model describes a network system stabilized by continuous tension rather than continuous compression units [27]. Thus, the mechanical stability of the network depends on the arrangements and re-arrangements of these components. One of the most typical tensegrity elements, the octahedral structure, is shown in Fig. 3. This basic structure consists of six rigid struts (compression-resisting elements) and 24 elastic cables (tensile-bearing elements). Depending on the experimental conditions, more complicated structures [70], viscoelastic cables [71], additional tensegrity elements and cables for nucleus and intermediate filaments [10,72], and multimodal or additional tensegrity elements [10,73,74] can be added.

The model correctly predicts the linear increase in the stiffness of the network with that of the applied stress in accordance with experimental results [27,56]. This model can also predict both static and dynamic behaviors of various cell types (e.g., human airway smooth muscle cells and the adherent cells) and has confirmed that the cells maintain their shape by redistributing and balancing the stress between the cytoskeleton and the extracellular matrix [31,32,56]. The pre-stress and subsequent increase in cell stiffness as predicted by this model can probably also explain the high elasticity and nonlinear viscoelastic behaviors observed in cells [32]. In contrast, this model still has a disadvantage in the prediction of the elastic modulus greater than experimentally measured values and a limitation in the description of cell viscoelastic behaviors, which requires con-

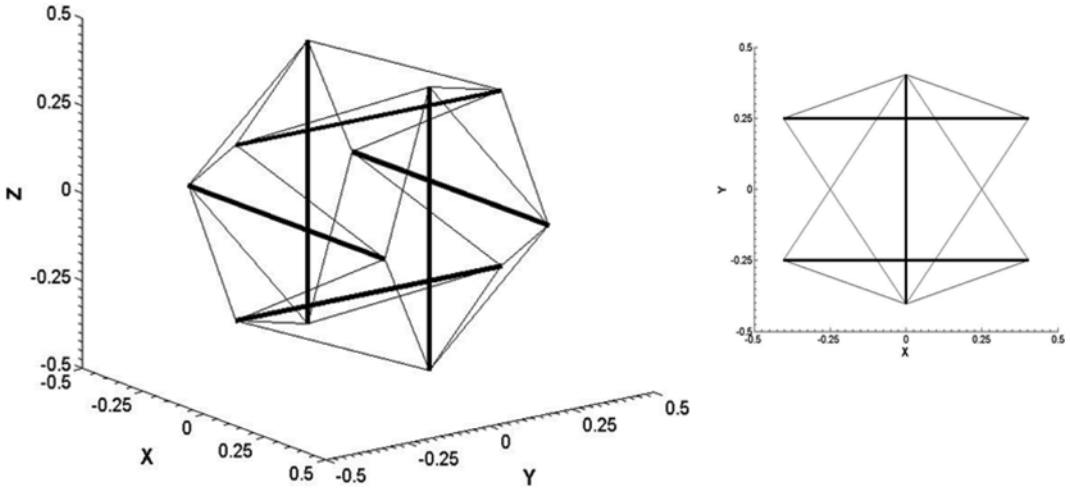

Fig. 3. A typical octahedron tensegrity element structure. The inset is a view from the xy-plane, which looks identical to the views from the zx-plane and the yz-plane (Redrawn from [71]).

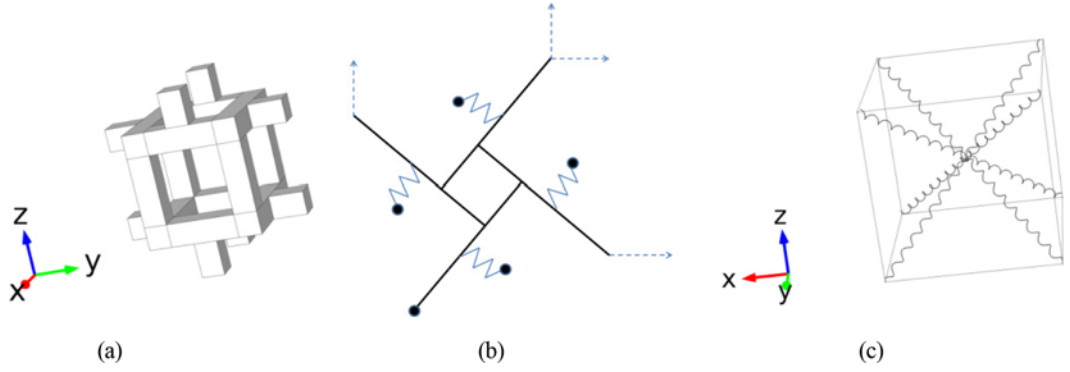

Fig. 4. The RVEs of (a) a typical open cell foam model (cuboid), (b) the semi-flexible polymer network model, and (c) the continuum polymer network models (8-chain model) (More details of each model are available in each original reference. Images were also redrawn [75,76,81]).

sideration of polymer structure at smaller scales [28,30].

4. Open Cell Foam Model

In this model, the actin network is a rigid cross-linking of beam-like structures, of which the shape is either cuboid, dodecahedron, tetrakaidecahedron, or icosahedron, with bending and twisting of the struts as the major stress-generating component. One of the typical stress units is a cuboid as shown in Fig. 4(a) [30,75]. This model has a major application when studying endothelial cells. It can also predict the strain hardening under compression for the adherent cells exposed to local mechanical perturbations [31]. The open cell foam model does not include pre-stress and thus does not explain the effect of stress on cell stiffness. The rigidity of the cross-link is a major disadvantage of the model, as in reality the actin cross-links are not rigid [12]. Overall, this model may not be able to provide as much information regarding cytoskeleton mechanics compared to the other models [30,31].

5. Semi-flexible Network Element Model

We named this model as the semi-flexible network element model because it describes the cytoskeleton rheological properties using an RVE-based approach to represent the structure of a semi-flexible polymer network [76]. As shown in Fig. 4(b), the RVE of this model consists of four equal-length strings and elastic springs, which simplifies the complex network structure. This model can predict Young's modulus as well as the shear modulus in terms of the relative ratio between the bending stiffness and the axial stiffness as well as the cross-link density. Although this model relates the microstructure of the cytoskeleton network to cell mechanical properties, it is not suitable for the simulation of cell dynamics due to the lack of structural information at larger scales (3D structure and microtubules) [30].

6. Continuum Polymer Network Model

The concept of this model is based on rubber elasticity in continuum mechanics; however, it also considers the force-extension relation of polymer chains, which is not directly included in the cell-scale continuum-based models. The RVE of this model is a continuous medium with principal stretch axes, as shown in Fig. 4(c). Different shaped RVEs have been used for describing polymer networks [77-80]. The eight-chain model or all-direction model was used for actin-filament networks [20,81].

This type of model has recently been improved to overcome the limitation of affine approximation and to include the prediction of negative normal stress behaviors. van Oosterwyck and co-

workers considered the inextensibility of chain and sliding cross-links for non-affine deformation [82]. Recently, two nonlinear springs connected in a series were used to show the effect of the linker stiffness on the rheological properties [83]. Unterberger and co-workers' nonaffine homogenization method can show the negative normal stress behavior [84,85]. A different approach, where a rigid rod connected to the surrounding elastic medium by cross-linkers, was reported to show the effect of the flexibility of the cross-link on the rheological properties [86].

Using a proper application of this model to the finite element method, the cell behavior, such as that observed in a microindentation experiment, can be simulated. However, only qualitative agreement was achieved, which is conjectured to be due to the lack of larger scale information as in the semi-flexible network element model [84,85].

7. Discussion on the Structure-based Models

The structure-based models provide a better understanding of the cytoskeleton behaviors and properties related to microstructural information, such as pre-stress and semi-flexibility, which are neglected in the cell-scale continuum-based models. But it is still an affine continuum approach and thus does not provide information about thermal fluctuations, network morphology, actin polymerization and cross-linking effects. The polymer-based model has been used to overcome those limitations, which will be discussed in the next section.

Although the structure-based models are more suitable for describing the cytoskeleton properties rather than the cell behaviors, the RVE approach is usually used when averaging over the cell and cannot be used for local fluctuations of deformations in a cell. However, proper choice of finite element method and multiscale simulation can allow structure-based models to simulate cell behaviors. For example, Chen used the tensegrity models to simulate cell spreading [87], and Unterberger and co-workers used the continuum polymer network model to simulate micropipette aspiration [84, 85]. However, the computational time is generally longer than that for continuum-based models due to the more complex calculations for each RVE.

Among the pre-stress models, the tensegrity model seems to be the best because it considers the actin networks as well as the microtubules, whereas other models do not consider the microtubules. Compared to the semi-flexibility models, the pre-stress models are generally better at describing larger cell scale behaviors due to the inclusion of the pre-stress. However, the semi-flexibility models are better in that more microstructural information (semi-flexibility) can be incorporated in simulating the cytoskeleton properties.

POLYMER-BASED MODELS (<1 μm)

We classify models which consider the structure of polymer molecules (actin filaments) or the morphology of polymer networks to predict cytoskeleton material properties as polymer-based models. The models in this type are further categorized into the discrete polymer network model (Mikado model) and the single polymer chain model. The original classification of the polymer-based model can be found in a review by Mackintosh [88] as well as one by Mofrad [13]. Recently, Unterberger and Holzapfel published a thorough review on polymer-based models in 2014 [28]. However, they also included the continuum polymer network model in their review. Here, we classify the continuum polymer network model as a structure-based model because the actin network structure is simplified into an RVE with chains in principal axes in a continuous medium.

The structure-based models utilize many imaginary microstructural units, which have been proposed to model the complex physical properties of cells. However, these models still lack actual information on the detailed structure and behaviors of the cytoskeleton at polymer molecular-level scales, such as cytoskeleton network morphology, cross-linker properties, and thermal fluctuation. Since the cytoskeleton is a complex structure of biopolymers, such as actin filaments, modeling the cytoskeleton structure at smaller polymer scales (~1 μm for polymer networks and <10 nm for single chains [28]) is essential to understand the origin of the unusual physical behaviors of cells. The polymer-based models have been used to elucidate the nonlinear mechanical response of the cytoskeleton to external forces in terms of collective behaviors (the effects of connectivity for networks and entanglements for solutions) as well as single chain properties (semi-flexibility and finite extensibility) of actin filaments.

The single polymer chain models provide the force-extension relationship of an actin filament, which is a fundamental aspect of all the models at larger scales. The discrete polymer network models are used to elucidate the interplay between the polymer network structure and the semi-flexibility of individual actin filaments. One of the distinguishing unusual behaviors of the cytoskeleton is the negative normal stress effect [89], which is explained only by polymer-based models that consider semi-flexibility.

1. Discrete Network Models

In this model, the RVE is a simulation box filled with cross-linked polymer chains. Each simulation method is different in how it simulates semi-flexible polymer chains, the properties of cross-linkers, and how to construct the network structure.

Simpler approaches include the 2D network models. Head and co-workers used random 2D networks of worm-like chains to derive the scaling of the bulk modulus and the affine/non-affine elastic deformation regime as a function of the concentration and contour length of an actin filament [90,91]. An elastic beam was used as the network element to predict the scaling of shear modulus [92]. A network of Euler-Bernoulli beams was employed to identify the elastic deformation regime according to the magnitude of strains [93]. The same network model was also used to explain the negative normal stress phenomenon with an asymmetric force-extension relation of actin filaments [94]. This model was also combined with a kinetic Monte Carlo method to show the strain dependence of the cross-link rupture and stiffness [95]. Alonso and co-workers proposed a model based on the flocking theory. Polymer chains are considered as point particles, while cross-linkers are represented as potential functions [96,97]. This model can simulate strain hardening, viscoelastic creep, stress relaxation, network rupture, and network reformation. Fallquivt and co-workers also used a 2D network model to study the effect of the filament length dispersion and the cross-linker compliance on the network material properties. They also performed a simulation using the con-

tinuum polymer network model to connect the effect of the cross-linker properties to a larger scale model [98].

Although 2D network approaches have been used for many studies, their limitations, such as the inability to represent the effect of 3D morphologies of cross-linkers on the actin network structure, have inspired the development of 3D network models. Huisman and co-workers have used the 3D network of Euler-Bernoulli beams [99] and an inextensible worm-like chain model [100,101] to study the strain-stiffening and scaling of elastic moduli. Brownian dynamics (BD) simulation method was used to study similar cytoskeleton network properties. Polymerization/depolymerization was simulated using actin monomers represented as rod-like units, which results in a 3D network structure [16,102,103]. Both the model by Huisman and the BD model [102] discovered that stress is concentrated in a few chains at high strain. The BD model was also used for extensive study of actin network behavior, such as identification of distinctive regimes and mechanisms of creep, as well as the origin and control of viscous flows in cortical cells [104]. The BD simulations and the dynamic cross-linking of the actin filaments can also be studied to understand the behavior of cancerous cells [105]. Whereas many models assume isotropic deformation, some models can predict the different morphologies of cytoskeleton networks, such as bundled filaments. The aforementioned BD model demonstrated the different morphologies as a function of cross-linker properties. Cyron and co-workers used stochastic governing equations to demonstrate different morphologies [106]. A recent study, which proposed a form-finding model (a 2D model was used earlier [107]), found that cells create parallel rather than disordered bundles of actin filaments during cell motion and cell adhesion. The parallel bundles align in the stretched direction, increasing the stiffness of the cell [108].

2. Single Polymer Chain Model

The single polymer chain model describes the most fundamental physical behaviors and properties of the cytoskeleton in the polymer molecule scale (<10 nm). Modeling the nonlinear force-stretch relationship of a single polymer chain is one the main issues in this type of model.

Molecular dynamics (MD) simulations are used for the smallest atomic scale. Matsushita and co-workers simulated a single F-actin filament with a full atomic structure to estimate its extensional stiffness [109]. Coarse-grained MD (CGMD) simulations were also performed by Chu and Voth to estimate the persistence length [110]. CGMD was also used to identify the heterogeneous mechanical properties of F-actin according to G-actin subunit structural differences [111-113].

The dynamics features of a single filament can be modeled at a larger scale (polymer chain level: ~10 nm) than the atomistic scale (~1 nm) in MD simulations. These types of models are called worm-like chain models. Although the atomic scale information can be scaled up [114] or modeled as an elastic rod that incorporates the helical structure of the filaments, the worm-like chain model [115, 116] has been widely used. Based on the previous analyses [88,90, 91], although a short filament with a length scale that is much smaller than its persistence length, its longitudinal response is determined by transverse thermal fluctuation. The model equation for the relationship between the force and the extension was later developed by Holzapfel and Ogden [117], and the Monte Carlo simulation was developed by Blundell and Terentjev [118]. There is also an approach using the finite element method to solve the Langevin equation for wormlike chain dynamics, which has also been extended to model 2D network behaviors [119].

3. Discussion on the Polymer-based Models

Consideration of polymer structure in models made it possible to predict or explain cytoskeleton properties/behaviors, which was not possible using larger scale models. For example, the frequency dependence of shear moduli, can be predicted by considering the polymer network structure, whereas the soft glassy model predicted that same behavior by adjusting a parameter [50]. The effects of cross-linkers are essential in determining the overall actin physical properties and the consequent cytoskeleton properties. The affinity of the actin binding proteins to the actin filament, the resulting network morphology (bundle or orthogonal), the degree of cross-linking, concentration, and the molecular weight affect the nonlinear viscoelastic response of the cytoskeleton [120,121].

However, the general disadvantages of considering microstructural information at smaller scales are heavy computational cost for larger scale simulation and the neglect of structural information at larger scales. Due to computational limits, the frequency dependence of shear moduli cannot be investigated for longer time ranges, and some filaments that are larger than the simulation box cannot be modeled [102]. The simulation of active behaviors, including polymerization/depolymerization of actin filaments, requires longer time scales. Polymerization/depolymerization can be considered only in the generation of a 3D network structure but not in the simulation of active behaviors [102,122]. However, Alonso and co-workers simulated active behaviors such as network reconstruction using a 2D model, which is computationally less costly [123].

It is understood that the behavior of the cytoskeleton network is not a function of one single component but is interdependent on the behaviors of all of the three major components together [10, 68]. Considering that, a model based solely on actin cannot predict and analyze the true cytoskeleton behavior. Similarly, these models also do not consider the compression in microtubules and the importance of intermediate filaments in bearing stress.

DISCUSSION/SUMMARY

We classified many mathematical and numerical models for mechanical behaviors and rheological properties of the cytoskeleton of a cell, which have been published up to 2014. The categories used are adapted from those used in a review by Mofrad in 2006: the cell-scale continuum-based model (originally continuum-based model), the structure-based model (tensegrity models and other RVE-based models), and the polymer-based model. These categories may be further classified into five groups by dividing the structure-based models into the pre-stress model and the semi-flexibility model as well as by dividing the polymer-based models into the single polymer chain model and the discrete polymer network model. Table 1 briefly summarizes the models we classified and discussed in this paper. The length scale classification is expected to promote a more systematic identification of the principles and characters of

Table 1. Summary of the cytoskeleton models

Models		Principle (how to model)		Advantage/Disadvantage	
Cell-scale continuum nodel (~10 μm)	Elastic/Viscoelastic model [13,36]	Cytoplasm as continuous media	Constitutive rheological equation	Good for cell dynamics simulation/ No microstructural information	Computationally efficient enough to describe the near equilibrium/transient behaviors of cell dynamics.
	Multiphasic model [41]		Constitutive rheological equations in each phase		More accurate at the cost of computational cost
	Soft Glassy Model [51]		Sollich's equation		Prediction over large time scale ranges
Structure-based Pre-stress model (4~10 μm)	Cortical Model and 2D/3D Cable Nets Model [56,57,61,63]	Pre-stressed stress unit	Cable networks	Pre-stress is considered. Possibility for both cell dynamics and cell properties. Lack of polymer structural information (semi-flexibility)	Lack of microtubule and intermediate filament information
	Tensegrity Model [10,56]		Cable-Strut networks		Considers all actin filaments, microtubules, and sometimes intermediate filaments. Versatility of the model
Structure-based Semi-flexibility model (1~4 μm)	Open Cell Foam Model [75]	Stress unit with semi-flexibility	Rigid beam structure	Semi-flexibility or bending is considered. Lack of microtubule and polymer molecule information (network morphology). Generally, not good for cell dynamics	Prediction of bending dominated deformation. Some structural information is not correct.
	Semi-flexibility Network Element Model [76]		Simplified oolymer network		Complex network behavior is well simplified. Lack of 3D structural information
	Continuum Polymer Network Model [81,84]		Continuous medium with principal axes		Continuum mechanics and microstructural strain-stretch relation are connected. Possibility for cell dynamics
Polymer-based discrete network model (10 nm~ 1 μm)	2D Networks [90,96]	Actin filament network	2D Networks of semi-flexible chains	Polymer morphology and collective network motions are considered. Not good for cell dynamics	Simpler than 3D. Active dynamics may be possible. Lack of 3D morphological information.
	3D Networks [16,99]		3D Networks of semi-flexible chains		Details of microstructural information are considered. Computational load limits active dynamics
Polymer-based single chain model (<10 nm)	Worm-like Chain Model [117]	Single actin filament chain	Continuous chain	Basic chain stretch dynamics. Not good for network properties and cell dynamics	Chain stretch dynamics considering semi-flexibility and finite inextensibility can be obtained
	Molecular Dynamics simulation [109,110]		G-actin monomer units		Basic parameters, persistence length and finite extensibility can be obtained

models.

The polymer-based models consider the stress elements, single polymer chain and polymer network at the smallest scales among the models in those categories. These models describe the relation between the cell properties and the molecular structure of the cytoskeleton. However, the high computational load prevents the use of

those models to simulate cell behavior. For example, the BD model [102] shows the limitations in the simulation of polymer chains longer than the simulation box, frequency range in the shear modulus prediction, and the simulation of structural rearrangement by polymerization/depolymerization. Additionally, the effects of the microtubules and the intermediate filaments, which are larger scale cellular components than actin filaments, are not included in the simulation box of actin networks.

The structure-based models describe the cytoskeleton properties and dynamic behavior using an RVE of imaginary stress elements, which coarse-grain the polymer chain and network behaviors. The semi-flexibility models connect the effects of semi-flexibility and the stiffness of polymer chains to cytoskeleton behavior at larger scales. The pre-stress models can explain the cell shape stability and the cell stiffness in terms of the pre-stress of the cytoskeleton, which is not considered in the cell-scale continuum-based model. The structure-based model can generally be used to model cytoskeleton material properties with better computational efficiency than the polymer-based models. However, they can also be used for cell dynamics with proper multi-scale numerical schemes. We also conjecture that models or studies which connect the pre-stressed model and the semi-flexibility model would make up for the disadvantages of both models.

The cell-scale continuum-based model, which handles the largest length scales among those model categories, can be used for modeling cell dynamics or behavior, which are associated with experiments on cell property measurements. The coarse-grained mathematical constitutive models cannot give information on cytoskeleton microstructure.

As we have reviewed, cytoskeleton modeling presents different challenges compared to usual entangled polymer system modeling, where smaller scale models based on microstructural information can describe polymer behavior and properties with more detail [124,125]. Due to the heterogeneity of the cytoskeleton network, models at smaller scales may lose larger scale structural information, such as the effects of pre-stress and microtubules. Therefore, the proper choice of models, especially for the structure-based models, as well as for multi-scale modeling or studies connecting models in different scales, is important. Furthermore, the development of a model using a new approach that employs coarse-graining to include more information from smaller scale studies to connect models should also be considered. For example, the mean-field approach used in stochastic models for simulating complex entangled polymer systems is being explored as a new interpretation of the cross-linking and rearrangement of networks [125].

In this review, we focused mainly on models based on the passive dynamics associated with pure mechanical/rheological responses. However, there are models based on different approaches, such as the gel-like model that was proposed by Pollock in which the cell movement and shape alteration can be described by the phase-transition mechanism of a gel-like structure [126]. There have been models that consider the active behaviors which are related to biological responses or structural rearrangement by polymerization/depolymerization. For example, the granular model considers microtubule rearrangement to describe cell crawling [127]. There have been models which described active behaviors of motor proteins [128] and growth and remodeling [129]. Although many reviews have pointed out the need to improve models for active dynamics [28,30,31], apparent barriers to that development include the inherent complexity of the models for passive dynamics and the need for broader interdisciplinary research including biomedical engineering, medical science, biophysics, biology, chemistry, materials science, and chemical engineering.

CONCLUDING REMARKS

This review provides a framework for approaching and understanding the plethora of biopolymer network models in terms of length scales, which are related to the stress components and the phenomena of interest. Identifying the length scale categories of a model can give quick insight into the advantages and disadvantages of the model, and the types of behaviors and properties described. Conversely, models can be selected based on the length scale of the phenomena of interest. The correct prediction of biopolymer network mechanical/rheological properties is important in many biomedical applications associated with biopolymer networks [1,130,131]. Therefore, the framework provided by this review is expected to promote various studies on biopolymer networks.

ACKNOWLEDGEMENT

The partial financial support from the Energy Research & Development Center of Missouri University of Science & Technology is gratefully acknowledged.

REFERENCES

1. D. Discher, C. Dong, J. J. Fredberg, F. Guilak, D. Ingber, P. Janmey, R. D. Kamm, G. W. Schimd-Scho and S. Weinbaulam, *Ann. Biomed. Eng.*, **37**, 847 (2009).
2. J. R. Stehn, N. K. Haass, T. Bonello, M. Desouza, G. Kottyan, H. Treutlein, J. Zeng, P. R. B. B. Nascimento, V. B. Sequeira, T. L. Butler, M. Allanson, T. Fath, T. A. Hill, A. McCluskey, G. Schevzov, S. J. Palmer, E. C. Hardeman, D. Winlaw, V. E. Reeve, I. Dixon, W. Weninger, T. P. Cripe and P. W. Gunning, *Cancer Res.*, **73**, 5169 (2013).
3. S. D. Bernal, S. B. Baylin, J. H. Shaper, A. F. Gazdar and L. B. Chen, *Cancer Res.*, **43**, 1798 (1983).
4. F. C. S. Ramaekers and F. T. Bosman, *J. Pathol.*, **201**, 351 (2004).
5. B. Geiger, J. Spatz and A. Bershadsky, *Nat. Rev. Mol. Cell Biol.*, **10**, 21 (2009).
6. M. Mehrbod and M. R. K Mofrad, *PLoS ONE*, **6**, 10, e25627 (2011).
7. E. M. Huisman, in *Introduction, Simulation of biopolymer networks under shear*, Leiden University, Leiden (2011).
8. M. E. Chicurel, C. S. Chen and D. E. Ingber, *Curr. Opin. Cell Biol.*, **10**, 232 (1998).
9. N. Wang, K. Naruse, D. Stamenovic, J. J. Fredberg, S. M. Mijailovich and I. M. Tolic-Norrelykke, *P. Natl. Acad. Sci. USA*, **98**, 7765 (2001).
10. D. E. Ingber, *J. Cell Sci.*, **116**, 1157 (2003).
11. C. Galli, S. Guizzardi, G. Passeri, G. M. Macaluso and R. Scandroglio, *Acta Biomedica.*, **76**, 5 (2005).
12. T. J. Chen, C. C. Wub and F. C. Su, *Med. Eng. Phys.*, **34**, 1375 (2012).

13. M. R. K. Mofrad, *Annu. Rev. Fluid Mech.*, **41**, 433 (2009).
14. H. Lodish, A. Berk, S. L. Zipursky, P. Matsudaira, D. Baltimore and D Darnell, *Molecular Cell Biology*, W. H. Freeman Co., Publications, New York (1999).
15. F. Gittes, B. Mickey, J. Nettleton and J. Howard, *J. Cell Biol.*, **120**, 923 (1993).
16. T. Kim, W. Hwang and R. D. Kamm, *Exp. Mech.*, **49**, 91 (2009).
17. M. L. Gardel, J. H. Shin, F. C. MacKintosh, L. Mahadevan, P. A. Matsudaira and D. A. Weitz, *Science*, **304**, 1301 (2004).
18. M. L. Gardel, J. H. Shin, F. C. MacKintosh, L. Mahadevan, P. A. Matsudaira and D. A. Weitz, *Phys. Rev. Lett.*, **93**, 188102 (2004).
19. F. C. MacKintosh, J. Kas and P. A. Janmey, *Phys. Rev. Lett.*, **75**, 4425 (1995).
20. C. Storm, J. J. Pastore, F. C. MacKintosh, T. C. Lubensky and P. A. Janmey, *Nature*, **435**, 191 (2005).
21. J. Xu, Y. Tseng and D. Wirtz, *J. Biol. Chem.*, **275**, 35886 (2000).
22. O. Lieleg, M. M. A. E. Claessen and A. R. Bausch, *Soft Matter*, **6**, 218 (2010).
23. B. Alberts, D. Bray, A. Johnson, J. Lewis, M. Raff, K. Roberts and P. Walter, in *Essential cell biology: An introduction to the molecular biology of the cell*, Garland Publishing, New York (1998).
24. I. Fujiwara, S. Takahashi, H. Tadakuma, T. Funatsu and S. Ishiwata, *Nat. Cell Biol.*, **4**, 666 (2002).
25. G. A. Buxton, N. Clarke and P. J. Husse, *Express Polym. Lett.*, **3**, 579 (2009).
26. T. Mitchison and M. Kirschner, *Nature*, **312**, 237 (1984).
27. D. Stamenović, *FME Transactions*, **34**, 57 (2006).
28. M. J. Unterberger and G. A. Holzapfel, *Biomech. Model Mechanobiol.*, **13**, 1155 (2014).
29. J. Chen, *Interface Focus*, **4**, 20130055 (2014).
30. T. J. Chen, C. C. Wu and F. C. Su, *Med. Eng. Phys.*, **34**, 1375 (2012).
31. M. M. Nava, M. T. Raimondi and R. Pietrabissa, *Biomech. Model Mechanobiol.*, **13**, 929, (2014).
32. E. Moeendarbary and A. R. Harris, *WIREs Syst. Biol. Med.*, **6**, 371 (2014).
33. S. S. Andrews, *Phys. Biol.*, **11**, 011001 (2014).
34. E. Roberts, *Cur. Opin. Struc. Biol.*, **25**, 86 (2014).
35. P. A. Janmey and C. Schmidt, in *Cytoskeletal Mechanics - Models and Measurements in Cell Dynamics*, M. R. K. Mofrad and R. D. Kamm Eds., Cambridge University Press (2006).
36. M. R. K. Mofrad, H. Karcher and R. D. Kamm, in *Cytoskeletal Mechanics - Models and Measurements in Cell Dynamics*, M. R. K. Mofrad and R. D. Kamm Eds., Cambridge University Press (2006).
37. B. Fabry, G. Maksym, J. Butler, M. Glogauer, D. Navajas and J. Fredberg, *Phys. Rev. Lett.*, **87**, 148102 (2001).
38. A. R. Bausch, F. Zeimann, A. A. Boulbitch, K. Jacobson and E. Sackmann, *Biophysics*, **75**, 2038 (1998).
39. D. Aubry, H. Thiam, M. Piel and R. Allena, *Biomech. Model Mechanobiol.* (2014), DOI:10.1007/s10237-014-0595-3.
40. I. Pajic-Lijakovic and M. Milivojevic, *Biomech. Model Mechanobiol.*, **13**, 1097 (2014).
41. F. Guilak, M. A. Haider, L. A. Setton, T. A. Laursen and F. P. T. Baaijens, in *Cytoskeletal Mechanics - Models and Measurements in Cell Dynamics*, M. R. K. Mofrad and R. D. Kamm Eds., Cambridge University Press (2006).
42. V. C. Mow, S. C. Kuei, W. M. Lai and C. G. Armstrong, *J. Biomech. Eng.*, **102**, 73 (1980).
43. W. M. Lai, J. S. Hou and V. C. Mow, *J. Biomech. Eng.*, **113**, 245 (1991).
44. W. Y. Gu, W. M. Lai and V. C. Mow, *J. Biomech. Eng.*, **120**, 169 (1998).
45. M. Biot, *J. Appl. Phys.*, **12**, 155 (1941).
46. A. F. Mak, *J. Biomech. Eng.*, **108**, 123 (1986).
47. M. R. DiSilvestro and J. K. Suh, *An. Biomed. Eng.*, **30**, 792 (2002).
48. F. P. T. Baaijens, W. R. Trickey, T. A. Laursen and F. Guilak, *An. Biomed Eng.*, **33**, 494 (2005).
49. L. Cao, F. Guilak and L. Setton, *Cell. Mol. Bioeng.*, **2**, 306 (2009).
50. B. Fabry and J. J. Fredberg, in *Cytoskeletal Mechanics - Models and Measurements in Cell Dynamics*, M. R. K. Mofrad and R. D. Kamm Eds., Cambridge University Press (2006).
51. B. Fabry and J. J. Fredberg, *Respir. Physiol. Neurobiol.*, **137**, 109 (2003).
52. P. Sollich, F. Lequeux, P. Hebraud and M. Cates, *Phys. Rev. Lett.*, **78**, 2020 (1997).
53. P. Sollich, *Phys. Rev. E*, **58**, 738 (1998).
54. M. Haider and F. Guilak, *J. Biomech. Eng.*, **122**(3), 236 (2000).
55. M. Haider and F. Guilak, *J. Biomech. Eng.*, **124**(5), 586 (2002).
56. D. Stamenović in *Cytoskeletal Mechanics - Models and Measurements in Cell Dynamics*, M. R. K. Mofrad and R. D. Kamm Eds., Cambridge University Press (2006).
57. D. V. Zhelev, D. Needham and R. M. Hochmuth, *Biophys. J.*, **67**, 696 (1994).
58. D. E. Discher, D. H. Boal and S. K. Boey, *Biophys. J.*, **75**, 1584 (1998).
59. S. K. Boey, D. H. Boal and D. E. Discher, *Biophys. J.*, **75**, 1573 (1998).
60. D. Stamenović and D. E. Ingber, *Biomech. Model Mechanobiol.,* **1**, 95 (2002).
61. M. F. Coughlin and D. Stamenović, *Biophys. J.*, **84**, 1328 (2003).
62. R. Paul, P. Heil, J. P. Spatz and U. S. Schwarz, *Biophys. J.*, **94**, 1470 (2008).
63. K. Y. Volokh and O. Vilnay, *Int. J. Solids Struct.*, **34**, 1093 (1997).
64. D. E. Ingber, L. Dike, L. Hansen, S. Karp, H. Liley and A. Manitos, *Int. Rev. Cytol.*, **150**, 173 (1994).
65. D. Stamenović and M. F. Coughlin, *J. Theor. Biol.*, **201**, 63 (1999).
66. F. J. Alenghat, B. Fabry, K. Y. Tsai, W. H. Goldmann and D. E. Ingber, *Biochem. Biophys. Res. Commun.*, **277**, 93 (2000).
67. J. M. Vasiliev, *J. Cell Sci. Suppl.*, **8**, 1 (1987).
68. D. E. Ingber, *Annu. Rev. Physiol.,* **59**, 575 (1997).
69. B. Fuller, *Portfolio & ARTnews Annual*, **4**, 112 (1961).
70. H. Baudriller, B. Maurin, P. Canadas, P. Montcourrier, A. Parmerggiani and N. Betache, *C R Mecanique*, **334**, 662 (2006).
71. P. Canadas, V. M. Laurent, C. Oddou, D. Isabey and S. Wendling, *J. Theor. Biol.*, **218**, 155 (2002).
72. N. Wang and D. Stramenovic, *Am. J. Physiol. Cell Physiol.,* **279**, C188 (2000).
73. D. E. Ingber, *FASEB J.*, **20**, 811 (2006).
74. Y. Z. Luo, X. Xu, T. Lele, S. Kumars and D. E. Ingber, *J. Biomech.*, **41**, 2379 (2008).
75. R. Satcher, C. F. Dewey Jr. and J. H. Hartwig, *Microcirculation*, **4**, 439 (1997).
76. S. Roy and H. J. Qi, *Phys. Rev. E.*, **77**, 061916 (2008).
77. P. J. Flory and J. Rehner Jr., *J. Chem Phys.*, **11**, 512 (1943).
78. L. R. G. Treloar, *Trans. Far. Soc.*, **42**, 83 (1946).

79. E. M. Arruda and M. C. Boyce, *J. Mech. Phys. Solids*, **41**, 389 (1993).
80. P. D. Wu and E. Giessen, *J. Mech. Phys. Solids*, **41**, 427 (1993).
81. J. S. Palmer and M. C. Boyce, *Acta Biomater.*, **4**, 597 (2008).
82. H. Van Oosterwyck, J. F. Rodriguez, M. Doblare and J. M. Garcia, *Comput. Methods Biomech. Biomed. Eng.*, **16**, 1002 (2013).
83. G. A. Holzapfel, M. J. Unterberger and R. W. Ogden, *J. Mech. Behav. Biomed. Mater.*, **38**, 78 (2014).
84. M. J. Unterberger, K. M. Schmoller, A. R. Bausch and G. A. Holzapfel, *J. Mech. Behav. Biomed. Mater.*, **22**, 95 (2013).
85. M. J. Unterberger, K. M. Schmoller, C. Wurm, A. R. Bausch and G. A. Holzapfel, *Acta Biomater.*, **9**, 7343 (2013).
86. C. P. Broederz, C. Storm and F. C. MacKintosh, *Phys. Rev. Lett.*, **101**, 118103 (2008).
87. T. J. Chen, C. C. Wu, M. J. Tang, J. S. Huang and F. C. Su, *PloS One*, **5**, e14392 (2010).
88. F. C. MacKintosh, in *Cytoskeletal Mechanics - Models and Measurements in Cell Dynamics*, M. R. K. Mofrad and R. D. Kamm Eds., Cambridge University Press (2006).
89. P. A. Janmey, M. E. McCormick, S. Rammensee, J. L. Leight, P. C. Georges and F. C. MacKintosh, *Nature Mater.*, **6**, 48 (2007).
90. D. A. Head, A. J. Levine and F. C. MacKintosh, *Phys. Rev. Lett.*, **91**, 108102 (2003).
91. D. A. Head, A. J. Levine and F. C. MacKintosh, *Phys. Rev. E Stat. Nonlin. Soft Matter Phys.*, **68**, 061907 (2003).
92. J. Wilhelm and E. Frey, *Phys. Rev. Lett.*, **91**, 108103 (2003).
93. P. R. Onck, T. Koeman, T. van Dillen and E. van der Giessen, *Phys. Rev. Lett.*, **95**, 178102 (2005).
94. E. Conti and F. C. MacKintosh, *Phys. Rev. Lett.*, **102**, 088102 (2009).
95. A. S. Abhilash, P. K. Purohit and S. P. Joshi, *Soft Matter*, **8**, 7004 (2012).
96. R. Alonso, J. Young and Y. Cheng, *Cell. Mol. Bioeng.*, **7**, 58 (2014).
97. F. Cucker and S. Smale, *IEEE Trans. Automat. Control*, **52**, 852 (2007).
98. B. Fallqvist, A. Kulachenko and M. Kroon, *J. Theor. Biol.*, **350**, 57 (2014).
99. E. M. Huisman, T. van Dillen, P. R. Onck and E. van der Giessen, *Phys. Rev. Lett.*, **99**, 208103 (2007).
100. E. M. Huisman, C. Storm and G. T. Barkema, *Phy. Rev. E*, **78**, 051801 (2008).
101. E. M. Huisman, C. Storm and G. T. Barkema, *Phys. Rev. E*, **82**, 061902 (2010).
102. T. Kim, W. Hwang, H. Lee and R. D. Kamm, *PLoS Comput. Biol.*, **5**, e1000439 (2009).
103. T. Kim, in *Thesis: Simulation of Actin cytoskeleton structure and rheology*, Massachusetts Institute of Technology, Massachusetts (2007).
104. T. Kim, M. L. Gardel and E. Munro, *Biophys. J.*, **106**, 526 (2014).
105. M. Mak, M. Zaman and R. Kamm, *Med. Phys.*, **41**, 164 (2014).
106. C. Cyron, A. R. Baush, K. W. Muller and W. A. Wall, *J. Comput. Phys.*, **244**, 236 (2013).
107. J. Gong, D. Zhang, Y. Tseng, B. Li, D. Wirtz and B. W. Scahfer, *PLoS ONE*, **8**, e77417 (2013).
108. B. Li, Y. Wang, J. Gong and J. Zhejiang, *Univ-Sci. A*, **15**, 732 (2014).
109. S. Matsushita, T. Adachi, Y. Inoue, M. Hojo and M. Sokabe, *J. Biomech.*, **43**, 3162 (2010).
110. J.-W. Chu and G. A. Voth, *Biophys. J.*, **90**, 1572 (2006).
111. O. N. Yogurtcu, J. S. Kim and S. X. Sun, *Biophys. J.*, **103**, 719 (2012).
112. J. Fan, M. G. Saunders and G. A. Voth, *Biophys. J.*, **103**, 1334 (2012).
113. J. Fan, M. G. Saunders, E. J. Haddadian, K. F. Ffreed, E. M. de la Cruz and G. a. Voth, *J. Mol. Biol.*, **425**, 1225 (2013).
114. D. Ming, Y. Kong, Y. Wu and J. Ma, *PNAS*, **100**, 104 (2003).
115. O. Kratky and G. Porod, *Recl. Trav. Chim. Pays-Bas.*, **68**, 1106 (1949).
116. M. Fixman and J. Kovac, *J. Chem. Phys.*, **58**, 1564 (1973).
117. G. A. Holzapfel and R. W. Ogden, *J. Elast.*, **104**, 319 (2011).
118. J. R. Blundell and E. M. Terentjev, *Macromolecules*, **42**, 5388 (2009).
119. Y. Lin, X. Wei, J. Qian, K. Y. Sze and V. B. Shenoy, *J. Mech. Phys. Solids*, **62**, 2 (2014).
120. B. Wagner, R. Tharmann, I. Haase, M. Fischer and A. R. Bausch, *PNAS*, **103**, 13974 (2006).
121. H. Hatami-Marbini and M. R. K. Mofrad, *Stud. Mechanobiology Tissue Eng. Biomater.*, **4**, 3 (2011).
122. G. A. Buxton, N. Clarke and P. J. Hussey, *eXPRESS Pol. Lett.*, **3**, 579 (2009).
123. R. Alonso, J. Young and Y. Cheng, *Cell. Mol. Bioeng.*, **7**, 58 (2014).
124. A. E. Likhtman, *J. Non-Newtonian Fluid Mech.*, **157**, 158 (2009).
125. J. Park, D. W. Mead and M. M. Denn, *J. Rheol.*, **56**, 1057 (2012).
126. G. H. Pollack, in *Cytoskeletal Mechanics - Models and Measurements in Cell Dynamics*, M. R. K. Mofrad and R. D. Kamm Eds., Cambridge University Press (2006).
127. B. Maurin, P. Canadas, H. Baudriller, P. Montcourrier and N. Bettache, *J. Biomech.*, **41**, 2036 (2008).
128. P. Chen and V. B. Shenoy, *Soft Matter*, **7**, 355 (2011).
129. S. Na, G. A. Meininger and J. D. Humphrey, *J. Theor. Biol.*, **246**, 87 (2007).
130. Y. Jang, S. Park and K. Char, *Korean J. Chem. Eng.*, **28**, 1149 (2011).
131. Y. Jeong and I. S. Kang, *Korean J. Chem. Eng.*, **12**, 540 (1995).